SUPPORTING INFORMATION

SI Materials and Methods

Animals. All experiments involving animals were approved by the University of Kentucky Institutional Animal Care and Use Committee (IACUC) and in accordance with the Association for Research in Vision and Ophthalmology (ARVO) Statement for the use of Animals in Ophthalmic and Visual Research. Mice were maintained on a constant 14:10 light-dark cycle. Water and food were provided ad libitum. Mice were sacrificed with CO_2 gas under constant gas flow. C57BL/6J wild-type, *Dicer1*$^{f/f}$, *Fas*$^{-/-}$, and *FasL*$^{-/-}$ mice (The Jackson Laboratory, Bar Harbor, ME) and *Casp8*$^{f/f}$ mice (1) were used for experiments. Cell-specific ablation of *Dicer1* and *Casp8* in mouse retinal pigmented epithelium (RPE) was performed by subretinal injection of an adeno-associated viral vector (AAV) coding for Cre recombinase under control of the *BEST1* promoter in *Dicer1*$^{f/f}$ and *Casp8*$^{f/f}$ mice, respectively.

Human tissue. Studies conformed to guidelines set forth in the Declaration of Helsinki. Donor eyes and ocular tissues from age-matched patients with or without geographic atrophy were obtained from various eye banks that had collected informed consent from donors. Diagnoses were confirmed by dilated ophthalmic examination before tissue acquisition before or after patient death. All geographic atrophy tissues had foveal involvement, and eyes were defined as normal if they showed no visible features of age-related macular degeneration (AMD). Cadaver specimens were de-identified, thus obviating the need for human subjects research approval.

Primary human RPE cell isolation and culture. RPE cells were isolated from human fetal eyes of 18–20 weeks gestation (Novogenixlabs, Los Angeles CA) by soaking the eyes in PBS containing 5% penicillin/streptomycin, cleaning off excess connective tissue, and removing the cornea, lens, vitreous, and retina. The RPE/choroidal/scleral tissue was placed in a 2% Dispase solution (Life Technologies, Grand Island, NY) in PBS for 20 min at 37 °C, mixed by pipetting up and down for 30 sec, and filtered by passing through a 70 μm, then a 40 μm filter. RPE cells were recovered by centrifugation and resuspended in Dulbecco's minimum essential medium (DMEM) supplemented with 2 mM L-glutamine, 100 U/mL penicillin, 100 μg/mL streptomycin (VWR International, West Chester, PA) containing at least 25% heat-inactivated fetal bovine serum (FBS; Irvine Scientific, Santa Ana, CA). The cells were first plated on laminin-coated plates until ready to be divided; no further coating was necessary and cells were grown in 10% DMEM. The cells were confirmed to be RPE cells by immunocytochemical positivity for cytokeratin (>95%) and the lack of immunoreactivity for endothelial-cell–specific von Willebrand factor (Dako, Carpinteria, CA) and glial fibrillary acidic protein (Chemicon, Temecula, CA). Cells were utilized from passage 2 to 4.

Immunolabeling and histology. Human eyes fixed in formalin were prepared as eyecups, embedded in paraffin and sectioned into 5 μm sections. Depigmentation was achieved using 0.25% potassium permanganate and 0.1% oxalic acid. Immunohistochemical staining was performed with the rabbit antibody against active (cleaved) Caspase-8 (1:3,000, Novus Biologicals), or control normal rabbit serum (1:3000, Jackson ImmunoResearch) to assess the specificity of the staining. Bound antibody was detected with biotin-conjugated secondary antibodies, followed by incubation with ABC reagent and visualized by Vector Blue (Vector

Laboratories). Levamisole (Vector Laboratories) was used to block endogenous alkaline phosphatase activity. Slides were washed in PBS and mounted in Vectamount (Vector Laboratories). Mouse retinal frozen sections (10-μm) and mouse RPE/choroid flat mounts were fixed with 2% PFA and stained with rabbit antibodies against mouse Caspase-8 (1:500; provided by Dr. R. Hakem, University of Toronto), mouse Zonula Occludens-1 (ZO-1) (1:100; Invitrogen) and mouse active Caspase-3 (1:200; Cell Signaling). For double staining of ZO-1 and Cre recombinase, flat mounts were stained with rabbit anti-mouse ZO-1 and mouse anti-Cre recombinase (1:500, Millipore) antibodies. Bound antibody was detected with Alexa594 and Alexa488-conjugated secondary antibodies (Invitrogen) and the sections were wet-mounted with ProLong anti-fade reagent with DAPI (Invitrogen). The RPE/choroid flat mounts were nuclear counterstained by Hoechst 33342 staining (Cell Signaling) and wet-mounted with ProLong anti-fade reagent. Images were captured using Leica SP-5 or Zeiss Axio Observer Z1 microscopes. Flat mount images of ZO-1 and active-Caspase-3 were acquired in a 1–2 mm region immediately surrounding, but not including, the subretinal injection site.

Assessment of RPE health by flat mount imaging. Healthy RPE cells form a uniform hexagonal "honeycomb" formation. RPE degeneration was assessed as a disruption of this uniform hexagonal sheet. Thus, RPE health was assessed as the presence or absence of morphological disruption in RPE flat mounts. Fisher's exact test was used to determine statistical significance.

Retinal morphology. To evaluate the morphology of the retina, hematoxylin and eosin staining was performed on frozen sections of mouse retina.

Immunoblotting. Mouse RPE/choroid tissue was lysed in protein lysis buffer (10 mM Tris base, pH 7.4, 150 mM NaCl, 1 mM EDTA, 1 mM EGTA, 1% Triton X-100, 0.5% NP-40, protease and phosphatase inhibitor cocktail (Roche)). Tissues were homogenized by sonication, followed by centrifugation at 12,000×*g* to separate out insoluble material. Protein was quantified by Bradford protein assay kit (Bio-Rad) with bovine serum albumin (BSA) as a standard. Protein lysates were run on NuPage Bis-Tris gels (Life Technologies) and transferred to Immun-Blot PVDF membranes (Bio-Rad). Blots were blocked for 1 h at room temperature and allowed to incubate in primary antibody solution specific against human Caspase-1 (1:500; Life Technologies), human Caspase-8 (1:1000; Cell Signaling), Vinculin (1:1000; Sigma-Aldrich), mouse Fas (1:200; Santa Cruz), and mouse Fas ligand (1:200; Santa Cruz) overnight at 4 °C. Appropriate horseradish peroxidase (HRP)-conjugated secondary antibodies were incubated with blots for 1 h at RT. Signal was visualized by enhanced chemiluminescence (ECL Plus) and imaged with VisionWorksLS Image Acquisition and Analysis Software (Version 6.7.2, UVP).

Subretinal injection. Subretinal injections (1 μl) were performed using a 35-gauge Exmire microsyringe (Ito Corporation). *In vivo* transfection of plasmid coding for Alu sequence (pAlu) or empty control vector (pNull) was achieved using 10% Neuroporter (Genlantis). AAV1-BEST1-Cre or AAV1-BEST1-GFP were injected at 1.0×10^{11} pfu/ml, *in vitro* transcribed *Alu* RNA at 0.3 mg/ml. Caspase-8 inhibitor (Z-IETD-FMK) or control peptide (Z-FA-FMK) (2 μg, R&D Systems, Minneapolis, MN) and recombinant mouse IL-18 protein (40 ng) were used for injection. Necrostatin-1 (400 μM) was administered as previously described (2).

Caspase-8 activity. Caspase-8 activity was quantified using a Caspase-8 fluorometric assay (R&D Systems). Cells or RPE/choroid lysates were harvested in the lysis buffer provided with the kit and the activity of caspase-8 was quantified in a flurometric assay following the manufacturer's instructions.

Electroretinography (ERG). Electroretinography was performed as previously described (3). Briefly, mice were dark adapted overnight, anesthetized, and both eyes were positioned within a binocular Ganzfeld stimulator (ColorDome; Diagnosys, Lowell, MA). After placing corneal and ground electrode, Espion software (Diagnosys) was used to deliver a fully automated flash intensity series, ranging from –5.0 to 1.0 log $cd \cdot s \cdot m^{-2}$.

Statistical analyses. Data analyzed with JMP 8.0 (SAS Software, Cary, NC) and expressed as mean ± SEM. Statistical significance was determined using two-tailed Student *t* or Fisher exact tests with $P < 0.05$. For fellow eye ERG measurements, paired analyses were performed.

Supplemental References

1. Salmena L*, et al.* (2003) Essential role for caspase 8 in T-cell homeostasis and T-cell-mediated immunity. *Genes & development* 17(7):883-895.
2. Murakami Y*, et al.* (2014) Programmed necrosis, not apoptosis, is a key mediator of cell loss and DAMP-mediated inflammation in dsRNA-induced retinal degeneration. *Cell death and differentiation* 21(2):270-277.
3. Yang Z*, et al.* (2008) Toll-like receptor 3 and geographic atrophy in age-related macular degeneration. *The New England journal of medicine* 359(14):1456-1463.

Supplemental Figures

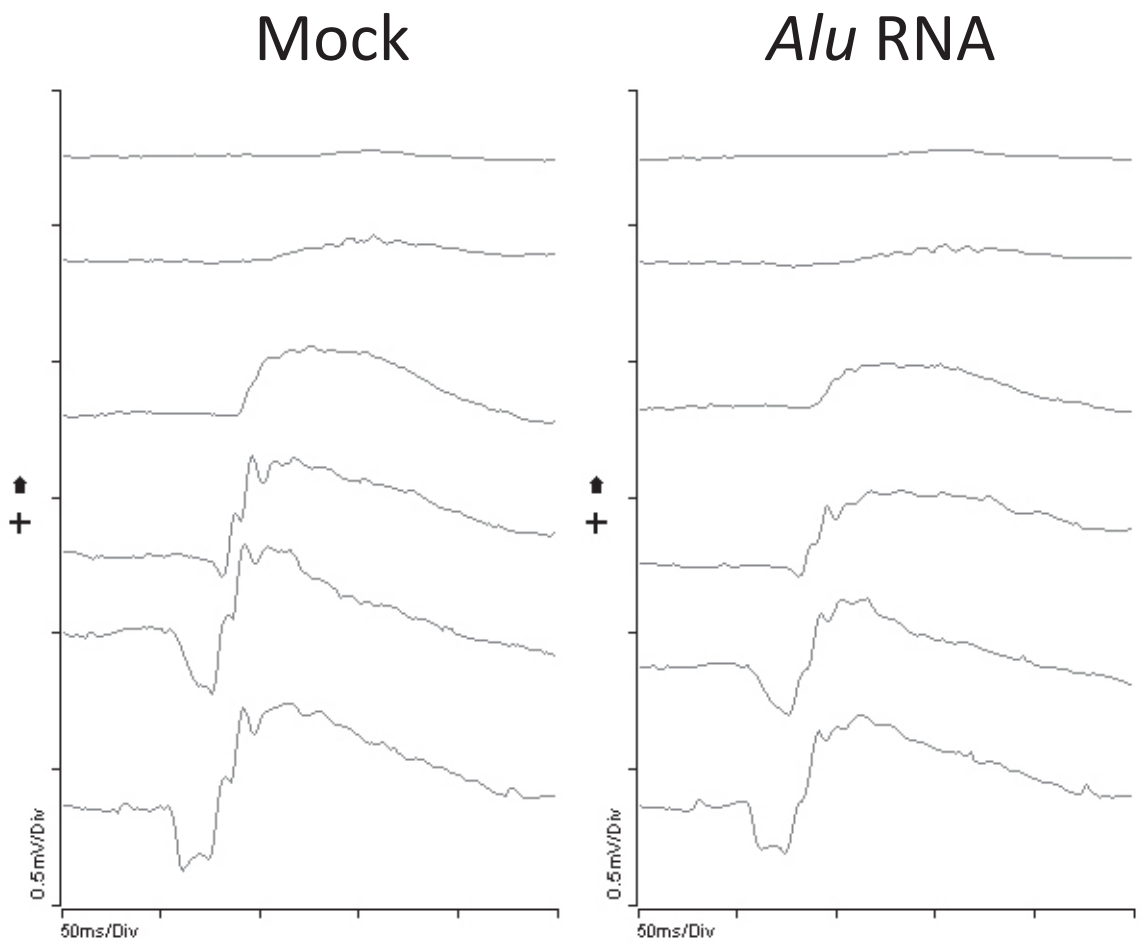

Fig. S1. *Alu* RNA suppresses retinal function. Subretinal injection of *Alu* RNA in wild-type mice causes a reduction in retinal electrical function as monitored by reduced scotopic flash electroretinography (ERG) amplitudes. Electrical traces of retina responses to increasing light intensities are shown in both mock- and *Alu* RNA-injected mice. Representative wave forms are shown. Images are representative of six independent experiments. Quantification of the maximum a-wave amplitude in Alu RNA-injected eyes, expressed as a ratio to that in PBS-injected contralateral eyes, showed it was reduced 0.83 ± 0.009 (Mean ± 95% C.I., N = 6, P = 0.014 by paired Student t test) (See Graph in Fig. S6).

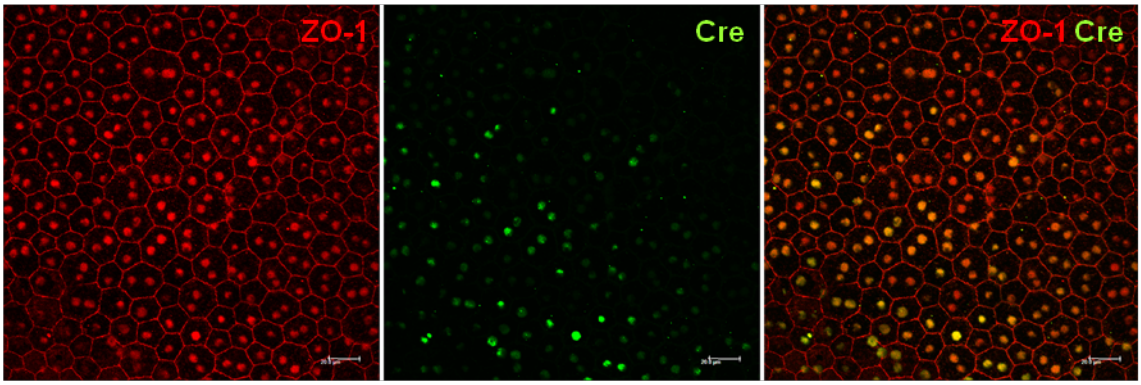

Fig. S2. Efficient AAV encoded Cre recombinase expression is not toxic to the mouse RPE. RPE flat mounts of wild-type mice subretinally injected with AAV1-BEST1-Cre show, at 2 weeks after injection, efficient nuclear expression of Cre recombinase (green), and a normal morphological appearance as assessed by ZO-1 (red) immunostaining. Images are representative of at least five independent experiments. Scale bars, 20 μm.

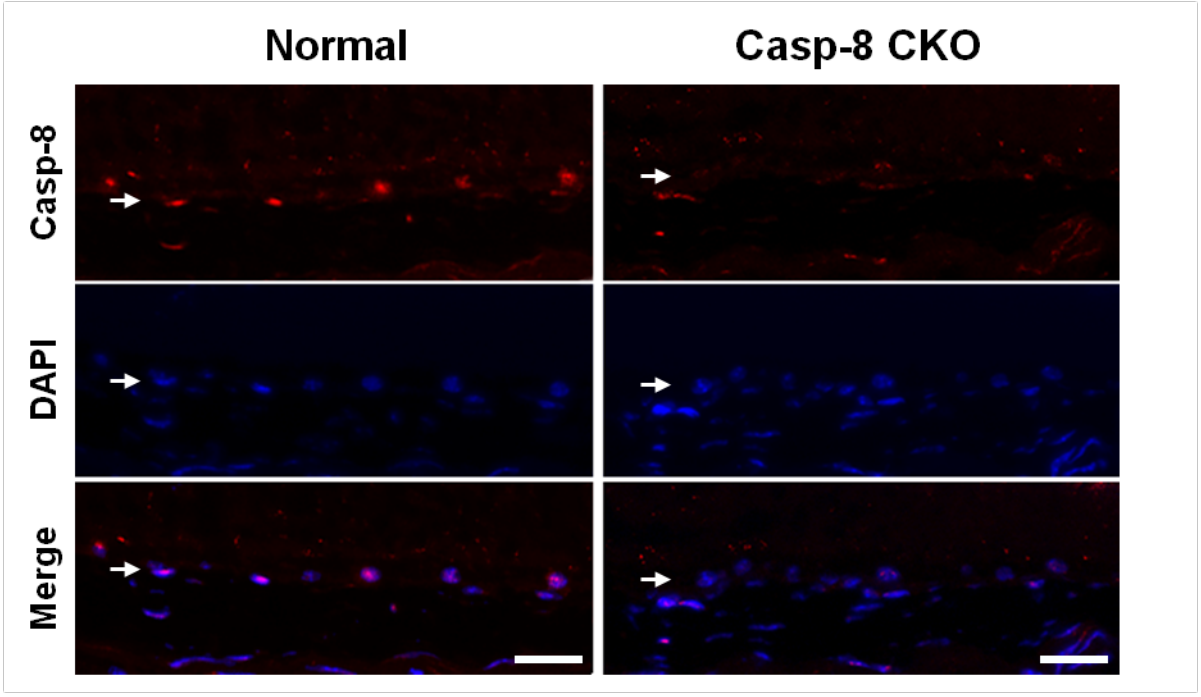

Fig. S3. Efficient knockdown of Caspase-8. Immunodetection of Caspase-8 showed substantial reduction of protein expression in *Casp8*$^{f/f}$ mice at 2 weeks following subretinal administration of AAV-BEST1-Cre in the area of injection (right panels) compared to uninjected areas (left panels). White arrows point to the RPE layers. Images are representative of at least three independent experiments. Scale bars, 20 μm.

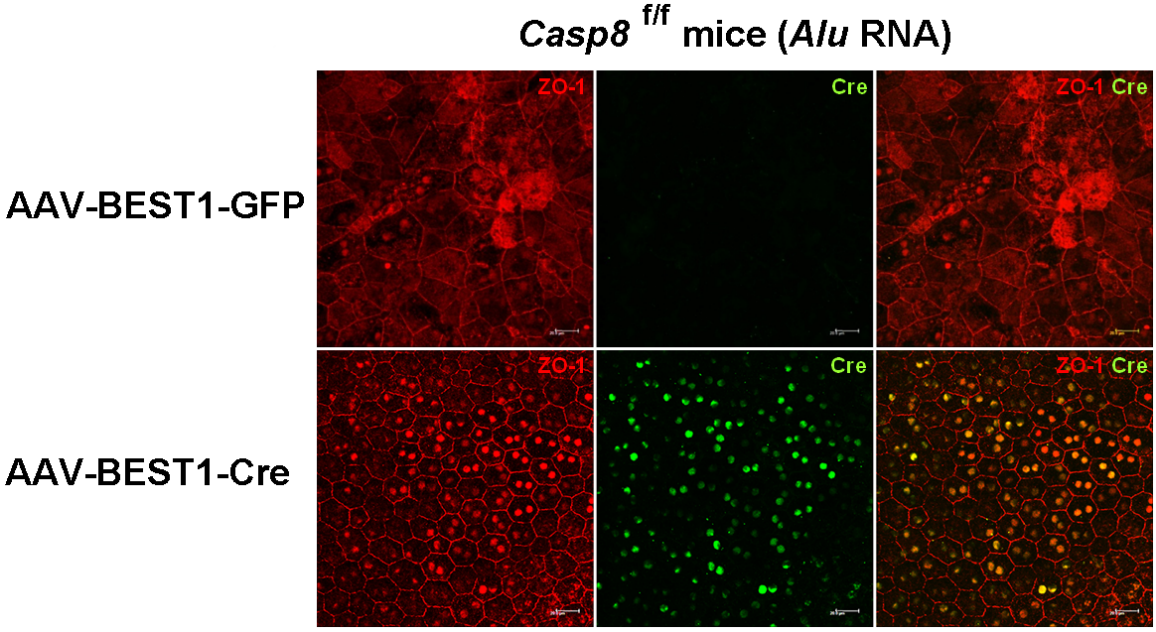

Fig. S4. Caspase-8 knockdown prevents *Alu* RNA-induced RPE degeneration. ZO-1 stained (red) RPE flat mounts show that subretinal administration of AAV-BEST1-Cre (bottom row), but not of AAV-BEST1-GFP (top row), in *Casp8*$^{f/f}$ mice protects against *Alu* RNA-induced RPE degeneration. N = 10, P = 0.008 by Fisher exact test. Representative images shown. Scale bars, 20 µm.

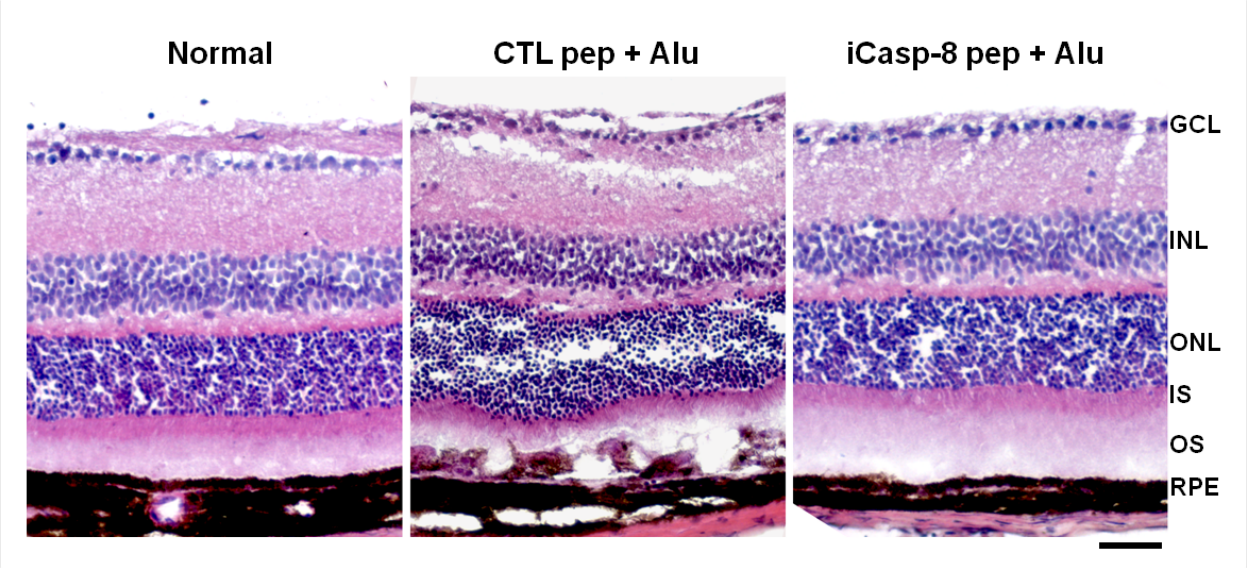

Fig. S5. Caspase-8 inhibition prevents *Alu* RNA-induced degeneration. Hematoxylin- and eosin-stained images show *Alu* RNA-induced disturbance of wild-type mouse RPE morphology is prevented by administration of a Caspase-8 inhibitory peptide (Z-IETD-FMK) but not by a control (CTL) peptide (Z-FA-FMK). An image of a normal uninjected mouse retina is shown for comparison. Images are representative of at least three independent experiments. Scale bars, 40 μm.

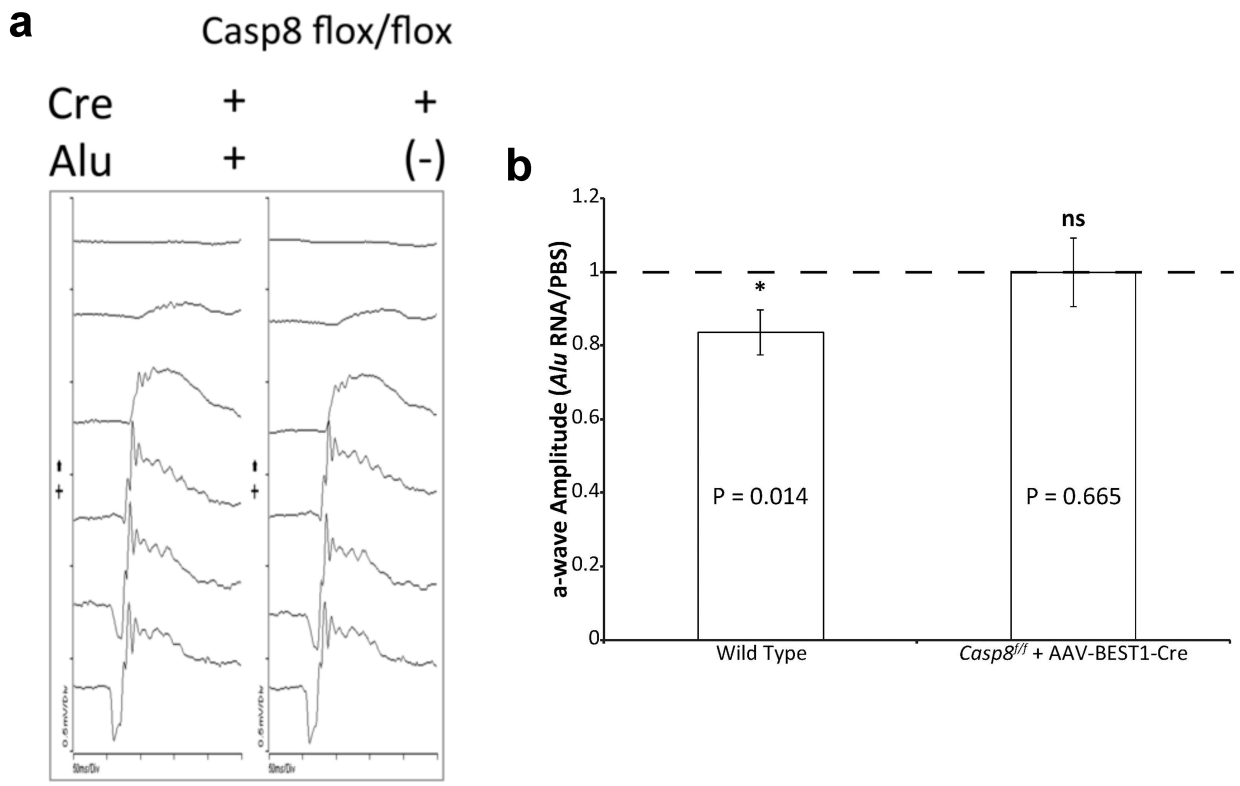

Fig. S6. Caspase-8 conditional genetic ablation protects against *Alu* RNA-induced loss of electrical function. (a, b) Subretinal injection of *Alu* RNA (+) in *Casp8*$^{f/f}$ mice following AAV1-BEST1-Cre injection does not cause a reduction in retinal electrical function, compared to mock injection (–) as monitored by reduced scotopic flash electroretinography (ERG) amplitudes. (a) Electrical traces of retina responses to increasing light intensities are shown in both mock- and *Alu* RNA-injected mice. Representative wave forms are shown. Images are representative of six independent experiments. (b) The maximum a-wave amplitude in *Alu* RNA-injected eyes, expressed as a ratio to that in PBS-injected contralateral eyes, is significantly different in wild-type mice (N = 6, P = 0.014 by paired Student t test) but not significantly different in AAV-BEST1-Cre-treated *Casp8*$^{f/f}$ mice (N = 6, P = 0.665 by paired Student t test). Mean ± 95% C.I. values shown.

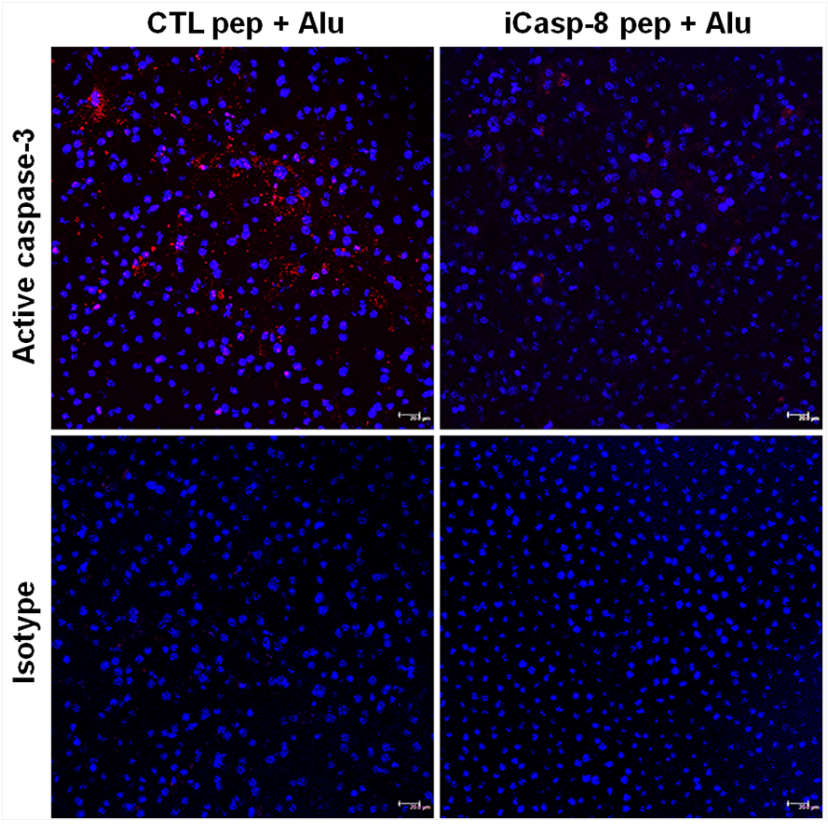

Fig. S7. Caspase-8 inhibition blocks Caspase-3 activation. Administration of a Caspase-8 inhibitory peptide (Z-IETD-FMK), but not control peptide (Z-FA-FMK), prevents activation of Caspase-3 (red, top row) by *Alu* RNA in wild-type mice as observed on RPE flat mounts. Specificity of immunolabeling revealed by absence of staining with isotype control antibody (bottom row). Nuclei stained blue with Hoechst 33342. Images are representative of at least three independent experiments. Scale bars, 20 μm.

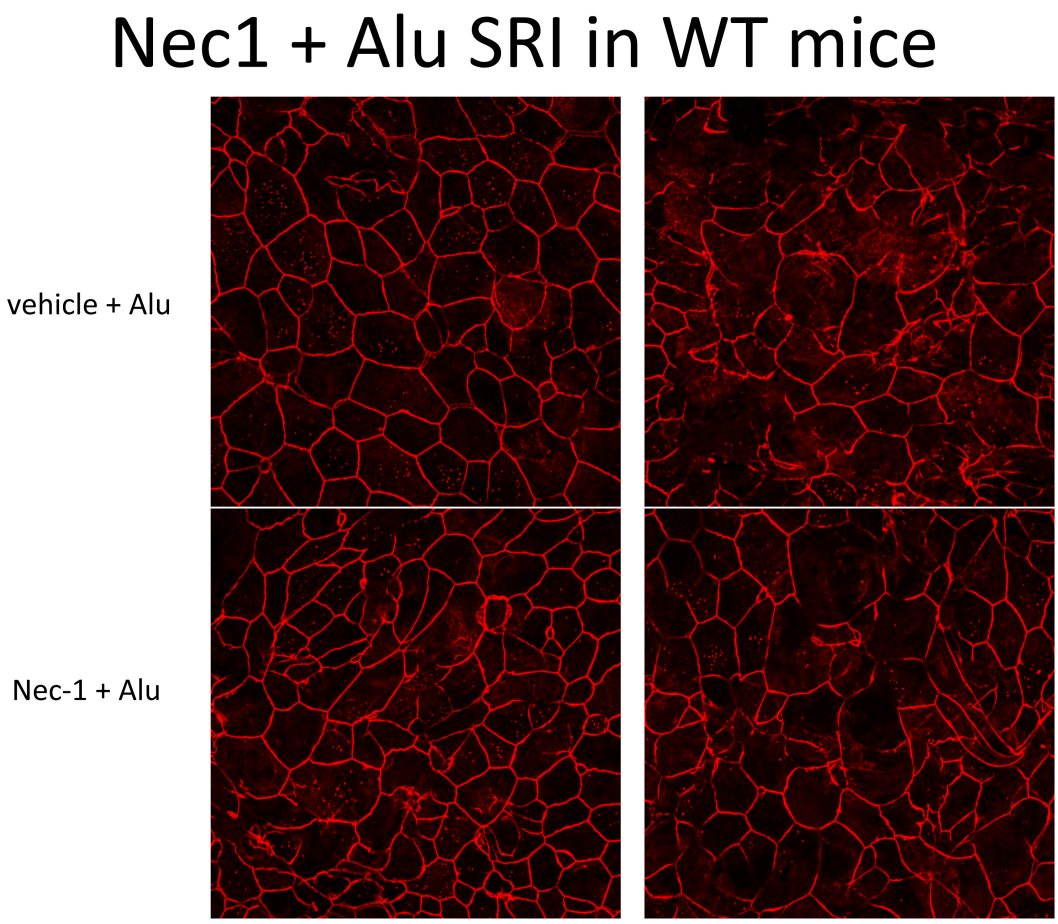

Fig. S8. *Alu* RNA does not induce RPE degeneration via necroptosis. Subretinal injection (SRI) of the necroptosis inhibitor Nec-1 (400 μM) or its vehicle did not protect the RPE against *Alu* RNA-induced RPE degeneration in wild-type mice as monitored by ZO-1 stained RPE flat mounts. N = 8. Necrostatin-1 was administered as described in Murakami et al., 2014 (2). Representative images shown.